Bonding Pattern Continuum from Covalent to Dative Carbon−Silicon Bonds for Substituted Silenes: A Theoretical Study

Mu-Jeng Cheng and San-Yan Chu*

Department of Chemistry, National Tsing Hua University, Hsinchu 30013, Taiwan

Received March 22, 2005

A quantum chemical B3LYP/cc-pVDZ study on bisubstituted silenes indicates that substitution at the carbon atom is more effective than that at the silicon atom at inducing a bent structure. π-Electron-donating substituents at the carbon atom drive the polarized π electrons toward the silicon atom. This reversed polarization effect induces bending of the silylene fragment. The local bending can be interpreted in terms of the second-order Jahn−Teller effect with the "transition density" of $\pi\sigma^*$ localized substantially at the Si atom. From the series of silenes having increasing bending of the SiH_2 unit, we have found that the structure of the SiH_2 fragment gradually shifts to a singlet silylene-like geometry. Thus, the covalently bonded SiH_2 fragments can evolve into datively bonded fragments of the singlet valence state in the bent silenes, which is a finding that is in accord with the CGMT model.

Introduction

The bonding and electronic structure of heavy analogues of olefins have received considerable attention in recent decades.[1−20] Carter and Goddard[21,22] and Malrieu and Trinquier[23,24] have interpreted the bond strength and the structure of $R_2X{=}YR_2$ species in terms of the valence states of the R_2X: and $:YR_2$ fragments; this approach is known as CGMT theory. Scheme 1 displays the two possible extreme bonding modes.

Scheme 1

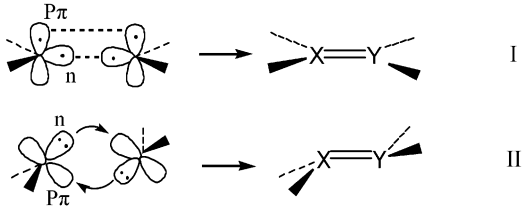

In the case of a low-lying triplet state of the divalent fragment having the $n^1p_\pi^1$ configuration, a normal planar double bond is formed between the two triplet fragments. This is the bonding mode I defined by Carter and Goddard to describe the bonding in most olefins.[21,22] On the other hand, when the singlet fragment $n^2p_\pi^0$ is significantly more stable, there is a tendency to bond directly from the two singlet fragments through a two-way donor−acceptor (n to p_π) interaction, as denoted by the two arrows. This is the bonding mode II defined by Malrieu and Trinquier to describes the bonding in disilenes and digermenes.[23,24]

The silenes (i.e., compounds containing a C═Si bond) provide an interesting intermediate case in which, from a naïve consideration for the mixed-row compounds, the bonding mode can, in principle, be either of type I or II. Recently, Ottosson demonstrated theoretically that π-electron-donating substituents on the carbon site cause substantial pyramidalization at the Si atom.[25,26] The substituent effect suppresses the natural $^{\delta-}C{=}Si^{\delta+}$ polarization effectively and induces the so-called "zwit-

* To whom correspondence should be addressed. E-mail: sychu@mx.nthu.edu.tw.

(1) Veszpremi, T.; Takahashi, M.; Ogasawara, J.; Sakamoto, K.; Kira, M. *J. Am. Chem. Soc.* **1998**, *120*, 2408.
(2) Sakamoto, K.; Ogasawara, J.; Sakurai, H.; Kira, M. *J. Am. Chem. Soc.* **1997**, *119*, 3405.
(3) Veszpremi, T.; Takahashi, M.; Hajgato, B.; Ogasawara, J.; Sakamoto, K.; Kira, M. *J. Phys. Chem. A* **1998**, *102*, 10530.
(4) Takahashi, M.; Sakamoto, K.; Kira, M. *Int. J. Quantum Chem.* **2001**, *84*, 198.
(5) Sakamoto, K.; Ogasawara, J.; Kon, Y.; Sunagawa, T.; Kabuto, C.; Kira, M. *Angew. Chem., Int. Ed.* **2002**, *41*, 1402.
(6) Leigh, W. J.; Boukherroub, R.; Kerst, C. *J. Am. Chem. Soc.* **1998**, *120*, 9504.
(7) Leigh, W. J.; Kerst, C.; Boukherroub, R.; Morkin, T. L.; Jenkins, S. I.; Sung, K. S.; Tidwell, T. T. *J. Am. Chem. Soc.* **1999**, *121*, 4744.
(8) Morkin, T. L.; Leigh, W. J. *Acc. Chem. Res.* **2001**, *34*, 129.
(9) Miracle, G. E.; Ball, J. L.; Powell, D. R.; West, R. *J. Am. Chem. Soc.* **1993**, *115*, 11598.
(10) Trommer, M.; Miracle, G. E.; Eichler, B. E.; Powell, D. R.; West, R. *Organometallics* **1997**, *16*, 5737.
(11) Power, P. P. *Chem. Rev.* **1999**, *99*, 3463.
(12) Driess, M.; Grutzmacher, H. *Angew. Chem., Int. Ed. Engl.* **1996**, *35*, 829.
(13) Chen, W. C.; Su, M. D.; Chu, S. Y. *Organometallics* **2001**, *20*, 564.
(14) Guliashvili, T.; El-Sayed, I.; Fischer, A.; Ottosson, H. *Angew. Chem., Int. Ed.* **2003**, *42*, 1640.
(15) El-Sayed, I.; Guliashvili, T.; Hazell, R.; Gogoll, A.; Ottosson, H. *Org. Lett.* **2002**, *4*, 1915.
(16) Avakyan, V. G.; Guselnikov, S. L.; Gusel'nikov, L. E. *J. Organomet. Chem.* **2003**, *686*, 257.
(17) Gusel'nikov, L. E. *Coord. Chem. Rev.* **2003**, *244*, 149.
(18) Gusel'nikov, L. E.; Avakyan, V. G.; Guselnikov, S. L. *J. Am. Chem. Soc.* **2002**, *124*, 662.
(19) Gusel'nikov, L. E.; Avakyan, V. G.; Gusel'nikov, S. L. *Russ. J. Gen. Chem.* **2001**, *71*, 1933.
(20) Bouhadir, G.; Bourissou, D. *Chem. Soc. Rev.* **2004**, *33*, 210.
(21) Carter, E. A.; Goddard, W. A. *J. Phys. Chem.* **1986**, *90*, 998.
(22) Carter, E. A.; Goddard, W. A. *J. Chem. Phys.* **1988**, *88*, 1752.
(23) Trinquier, G.; Malrieu, J. P.; Riviere, P. *J. Am. Chem. Soc.* **1982**, *104*, 4529.
(24) Trinquier, G.; Malrieu, J. P. *J. Am. Chem. Soc.* **1987**, *109*, 5303.

10.1021/om050221j CCC: $30.25
Publication on Web 06/16/2005

Scheme 2

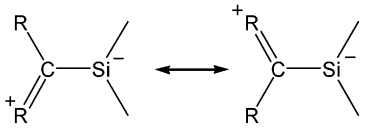

Scheme 3

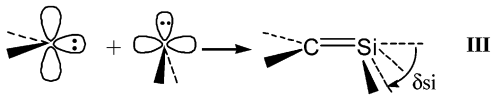

terionic resonance" structure presented in Scheme 2. Apeloig and Karni analyzed such reversed polarity of the π bond (i.e., $^{\delta+}C{=}Si^{\delta-}$) from calculations performed at the Hartree−Fock level and proposed that it is the most important electronic factor that enhances the kinetic stability of silenes.[27] Most known silenes are transient species that have very short lifetimes, but, using this electronic stabilization effect and additional sterically encumbered protecting groups, in 1981 Brook et al. isolated the first stable silenes, which possessed the general formula $(Me_3Si)_2Si{=}CR(OSiMe_3)$.[28,29] An understanding and utilization of reversed polarization has been crucial to the development of silene chemistry.[25,27,30]

It appears that the bonding model corresponding to those zwitterionic resonances in Scheme 2 having a pyramidal Si atom can be represented by bonding mode III (Scheme 3), in which the singlet carbene fragment donates its lone pair of electrons in its n orbital to the vacant p_π orbital of the singlet silylene fragment. In turn, the singlet carbene fragment has partial π-bond character with its substituents presented as displayed in the resonance structures in Scheme 2. We note that the C−Si singlet bond in the resonance structure actually corresponds to the dative C−Si bond in bonding mode III.

Mode III differs from mode II in that there is only a one-way donor−acceptor interaction, and thus, n(Si) to p_π(C) back-bonding is not important. This bonding mode has been discussed previously for silylene-isocyanide complexes[31,32] and silastannene.[33] Lee and Sekiguchi named the bonding modes II and III as symmetrical and unsymmetrical donor−acceptor interactions, respectively.[33] In fact, bonding mode III represents an extreme case. The substituent effect can give rise to a continuous variation between modes I and III—the covalent and one-way dative bonding modes, respectively—as indicated by the magnitude of the increasing folding angle (δ_{Si}) of the silylene fragment or the extent of Si pyramidalization as indicated by the value of $\sum\theta_{Si}$ (see the footnotes of Table 2). The carbene side is nearly planar, however, and has a small folding angle, δ_C. This interesting bonding variation arising from the substituent effect became the focus of our present study.

Our interest in this area was to provide some rationalization for the geometry observed for bonding mode III. We describe our study of this bending in a stepwise manner. First of all, we demonstrate that the substituent effect on the carbon atom polarizes the C−Si π bond toward the silicon atom in an enforced planar geometry. Subsequently, such reversed polarization of the π electrons leads to bending of the silylene fragment at the silicon site. Finally, for a series of silenes of increasing folding angles δ_{Si}, we demonstrate that the geometry of the SiH_2 fragment gradually shifts in the bent molecules to that of the singlet silylene-like structure. Therefore, this phenomenon is a clear manifestation of the CGMT model when applied to heteronuclear silenes.

2. Computational Details

The theoretical calculations reported in this paper were performed using density functional theory at the B3LYP/cc-pVDZ level[34−36] implemented in the Gaussian 98 program.[37] Substitution at either the silicon (**1**) or carbon (**2**) atom of the double bond was examined (Scheme 4). The set of silenes we considered was much smaller than that studied by Ottosson,[25] who considered variations of X, Y, and Z in the singlet series $XYC{=}SiZ_2$. Apeloig and Karni have demonstrated that monosubstituted silenes of the types $RHSi{=}CH_2$ and $H_2Si{=}CHR$ (R = H, CH_3, SiH_3, OH, $OSiH_3$, F, CN, and NO_2) all have planar structures when analyzed at the Hartree−Fock level.[27] Ottosson, however, found that some monosubstituted silenes, such as $(NH_2)HC{=}SiH_2$, possess bent structures when studied at the B3LYP/6-31+G(d) level of theory. In this paper, we consider only the disubstituted compounds to provide compatibility with the results obtained for the ring compounds in the set. The ring compounds we chose are models of those reported by Kira et al.[5] and Lappert et al.[38] Moreover, we restrict our substituents to π donors to take advantage of the important reversed polarization effect.

3. Results and Discussion

3.1. Structure. Table 1 lists selected geometric parameters that we obtained from calculations of the planar silenes (i.e., **1** and **2**). The harmonic vibrational frequency calculations indicate that the planar structures of **2b**−**d**, **2h**, and **2i** are the transition states for the inversion motion between a pair of trans-bent structures, while the other planar structures are minima.

(25) Ottosson, H. *Chem. Eur. J.* **2003**, *9*, 4144.
(26) El-Nahas, A. M.; Johansson, M.; Ottosson, H. *Organometallics* **2003**, *22*, 5556.
(27) Apeloig, Y.; Karni, M. *J. Am. Chem. Soc.* **1984**, *106*, 6676.
(28) Brook, A. G.; Abdesaken, F.; Gutekunst, B.; Gutekunst, G.; Kallury, R. K. *J. Chem. Soc. Chem. Commun*. **1981**, 191.
(29) Brook, A. G.; Nyburg, S. C.; Abdesaken, F.; Gutekunst, B.; Gutekunst, G.; Kallury, R. K. M. R.; Poon, Y. C.; Chang, Y. M.; Wongng, W. *J. Am. Chem. Soc.* **1982**, *104*, 5667.
(30) Bendikov, M.; Quadt, S. R.; Rabin, O.; Apeloig, Y. *Organometallics* **2002**, *21*, 3930.
(31) Takeda, N.; Kajiwara, T.; Suzuki, H.; Okazaki, R.; Tokitoh, N. *Chem. Eur. J.* **2003**, *9*, 3530.
(32) Takeda, N.; Suzuki, H.; Tokitoh, N.; Okazaki, R.; Nagase, S. *J. Am. Chem. Soc.* **1997**, *119*, 1456.
(33) Lee, V. Y.; Sekiguchi, A. *Organometallics* **2004**, *23*, 2822.
(34) Becke, A. D. *J. Chem. Phys.* **1993**, *98*, 5648.
(35) Stephens, P. J.; Devlin, F. J.; Chabalowski, C. F.; Frisch, M. J. *J. Phys. Chem.* **1994**, *98*, 11623.
(36) Woon, D. E.; Dunning, T. H. *J. Chem. Phys.* **1993**, *98*, 1358.
(37) Frisch, M. J.; Trucks, G. W.; Schlegel, H. B.; Scuseria, G. E.; Robb, M. A.; Cheeseman, J. R.; Zakrzewski, V. G.; Montgomery, J., J. A.; Stratmann, R. E.; Burant, J. C.; Dapprich, S.; Millam, J. M.; Daniels, A. D.; Kudin, K. N.; Strain, M. C.; Farkas, O.; Tomasi, J.; Barone, V.; Cossi, M.; Cammi, R.; Mennucci, B.; Pomelli, C.; Adamo, C.; Clifford, S.; Ochterski, J.; Petersson, G. A.; Ayala, P. Y.; Cui, Q.; Morokuma, K.; Malick, D. K.; Rabuck, A. D.; Raghavachari, K.; Foresman, J. B.; Cioslowski, J.; Ortiz, J. V.; Stefanov, B. B.; Liu, G.; Liashenko, A.; Piskorz, P.; Komaromi, I.; Gomperts, R.; Martin, R. L.; Fox, D. J.; Keith, T.; Al-Laham, M. A.; Peng, C. Y.; Nanayakkara, A.; Gonzalez, C.; Challacombe, M.; Gill, P. M. W.; Johnson, B.; Chen, W. C.; Wong, M. W.; Andres, J. L.; Gonzalez, C.; Head-Gordon, M.; Replogle, E. S.; Pople, J. A.; *Gaussian 98*; Pittsburgh, PA, 1998.
(38) Boesveld, W. M.; Gehrhus, B.; Hitchcock, P. B.; Lappert, M. F.; Schleyer, P. V. R. *Chem. Commun.* **1999**, 755.

Table 1. B3LYP/cc-pVDZ-Derived Data for Selected Geometrical Parameters (Å, deg) of the Planar Silenes (see Scheme 4) and Triplet−Singlet Energy Gaps for the SiR_2 and CR_2 Fragments

	$H_2C{=}SiR_2$ (**1**)							
compound	R_{C-Si}	R_{C-H}	R_{Si-R}	∠HCH	∠RSiR	ΔE_{ST}[a]	$\Delta\Delta E_{ST}$[b]	$\Sigma\Delta E_{ST}$[c]
1a	1.716	1.094	1.487	115.9	115.0	20.4	0.0	8.1
1b	1.687	1.090	1.627	119.5	106.2	74.3	53.9	62.0
1c	1.700	1.092	1.664	117.4	103.1	63.4	43.0	51.1
1d	1.707	1.092	1.732	116.9	106.5	55.4	35.0	43.1
1e	1.699	1.091	2.063	119.0	110.2	53.9	33.5	41.6
1f	1.709	1.092	2.148	117.5	106.4	44.2	23.8	31.9
1g	1.721	1.094	2.276	116.1	118.6	27.2	6.8	14.9
1h	1.707	1.091	1.741	118.1	90.9	58.4	38.0	46.1
1i	1.706	1.091	1.808	119.1	44.2	83.8	63.4	71.5
	$R_2C{=}SiH_2$ (**2**)							
compound[d]	R_{C-Si}	R_{Si-H}	R_{C-R}	∠HSiH	∠RCR	ΔE_{ST}[a]	$\Delta\Delta E_{ST}$[b]	$\Sigma\Delta E_{ST}$[c]
2a	1.716	1.487	1.094	115.9	115.0	−12.3	0.0	8.1
2b^0	1.745	1.476	1.333	123.2	109.8	52.6	**64.9**	**73.0**
2c^0	1.753	1.479	1.371	120.9	114.5	50.5	**62.8**	**70.9**
2d^0	1.775	1.481	1.402	121.6	110.5	52.8	**65.1**	**73.2**
2e	1.741	1.480	1.751	120.5	114.7	18.3	30.6	38.7
2f	1.741	1.484	1.792	117.6	119.1	27.6	39.9	48.0
2g	1.735	1.488	1.848	116.0	113.2	8.8	21.1	29.2
2h^0	1.803	1.477	1.388	125.1	102.9	83.5	**95.8**	**103.9**
2i^0	1.730	1.481	1.459	120.0	53.6	69.1	**81.4**	**89.5**

[a] Values of E(triplet) − E(singlet) for the SiR_2 fragments for type **1** molecules and CR_2 for the type **2** molecules, obtained from restricted B3LYP calculations. [b] Values of $\Delta E_{ST}(SiR_2) - \Delta E_{ST}(SiH_2)$ for type **1** compounds and $\Delta E_{ST}(CR_2) - \Delta E_{ST}(CH_2)$ for type **2** compounds. [c] Values of $\Delta E_{ST}(SiR_2) + \Delta E_{ST}(CH_2)$ for type **1** compounds and $\Delta E_{ST}(SiH_2) + \Delta E_{ST}(CR_2)$ for type **2** compounds. [d] The symbol **2x**^{0} represents the enforced planar conformation for the fully optimized molecule **2x** of bent geometry (Table 2).

Table 2. B3LYP/cc-pVDZ-Derived Data for Selected Geometric Parameters (Å, deg) of the trans-Bent Silenes and Their Inversion Barriers (kcal/mol)

	R_{C-Si}	R_{Si-H}	R_{C-R}	∠HSiH	∠RCR	$\Sigma\theta_C$[a]	$\Sigma\theta_{Si}$[a]	δ_C[b]	δ_{Si}[b]	E_a[c]
2b	1.790	1.489	1.325	115.8	109.0	357.9	334.1	12.9	51.8	1.2 (1.0)
2c	1.849	1.504	1.344	108.5	115.7	358.6	313.0	11.5	68.7	2.9 (2.7)
2d	1.950	1.533	1.343	98.4	116.4	359.4	284.8	7.6	85.1	13.4 (13.7)
2h	1.946	1.535	1.363	97.9	103.1	358.9	282.8	8.9	86.3	20.6 (19.6)
2i	1.808	1.504	1.441	108.8	54.7	354.1	319.8	13.5	62.6	3.5 (3.2)

[a]

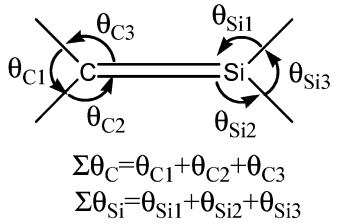

$\Sigma\theta_C = \theta_{C1} + \theta_{C2} + \theta_{C3}$

$\Sigma\theta_{Si} = \theta_{Si1} + \theta_{Si2} + \theta_{Si3}$

[b]

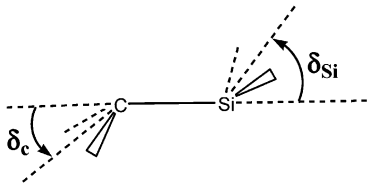

[c] E_a = E(planar) − E(trans-bent). The values with zero-point vibrational energy (ZPVE) corrections are given in parentheses.

Therefore, we use the symbols **2b**^{0}, **2c**^{0}, **2d**^{0}, **2h**^{0}, and **2i**^{0} to denote the enforced planar structures of these compounds. Substitution at silicon (i.e., **1**) shortens the C=Si bond relative to that of the parent $H_2C{=}SiH_2$, whereas substitution at carbon (i.e., **2**) causes elongation. Ottosson[25,26] observed a similar result, as did Apeloig and Karni[27] for a series of monosubstituted silenes. These results can be rationalized in terms of a substitutent effect on the bond polarity for type **1** compounds: the electronegative substituents enhance the polarization of the C−Si bond in $H_2C{=}SiR_2$ such that the silicon atom becomes more positively charged and the carbon atom more negatively charged. The C=Si bond is expected to shorten as a result of this increase in bond polarity. For type **2** compounds, elongation of the C=Si bond supports the important contribution of the "zwitterionic resonance" structure presented in Scheme 2. We studied 11 compounds (**1x** and **2x**, **x** = **a**, **b**, **c**, **d**, **e**, **f**) in common with Ottosson. In general, the deviations in C=Si bond distance in Å between our results and his are in the third decimal place for the planar compounds and the second decimal place for the bent compounds (**1a**, **1c**, and **1d**).

Table 1 lists the values of ΔE_{ST} ($E_{Triplet} - E_{Singlet}$) for the substituted carbenes (CR_2) and silylenes (SiR_2); generally, for the same substitutent, the latter have larger values of ΔE_{ST} than do the former. We find that the quantity $\Delta\Delta E_{ST}$, the difference in ΔE_{ST} with respect

Scheme 4

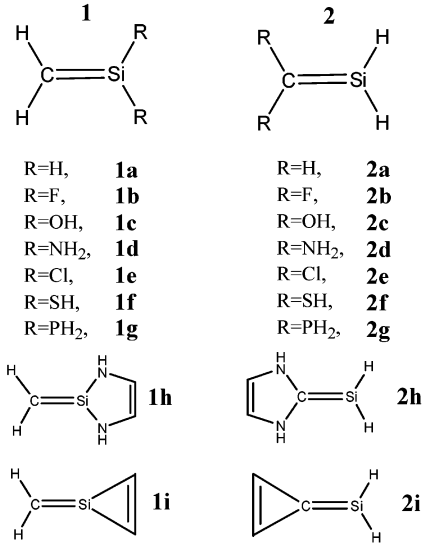

to the unsubstituted carbene (CH_2), is informative (see the discussion below).

$$\Delta\Delta E_{ST} = \Delta E_{ST}(CR_2) - \Delta E_{ST}(CH_2) \quad (1)$$

We also define a similar quantity for the substituted silylene. The value of $\Delta\Delta E_{ST}$ can display the difference in π-electron-donating capability for the same substituent with respect to different central atoms. For example, the values of $\Delta\Delta E_{ST}$ for $(NH_2)_2C$ and $(NH_2)_2Si$ are 65.1 and 35.0 kcal/mol, respectively. Therefore, the NH_2 substituent is a far more influential substituent for the carbene than it is for the silylene for providing the π-donating effect. This effect, however, is not obvious from the corresponding values of ΔE_{ST}, which are 52.8 and 55.4 kcal/mol, respectively. We find that the first-row substituents—F, OH, $(CH)_2$, and $(NHCH)_2$—are also stronger π-donating substituents for carbenes than they are for silylenes, as indicated by the larger values of $\Delta\Delta E_{ST}$ in the carbene series. In contrast, the second-row substituents—Cl, SH, and PH_2—are comparable for both carbenes and silylenes; their weak π-donor ability is indicated by the similarly small values of $\Delta\Delta E_{ST}$ in these two series. This finding reflects the simple fact that the π bonds within the first-row elements are stronger than those either within the second-row elements or between the first- and second-row elements. The π bond here refers to the donor−acceptor type, rather than that of the regular covalent bond.

We also consider the quantity $\sum\Delta E_{ST}$, which Trinquier et al. used previously,[23,24] as a measure of the bent distortions of multiple bonds:

$$\sum\Delta E_{ST} = \Delta E_{ST}(SiR_2) + \Delta E_{ST}(CH_2) \text{ for compounds } \mathbf{1} \quad (2)$$

$$\sum\Delta E_{ST} = \Delta E_{ST}(CR_2) + \Delta E_{ST}(SiH_2) \text{ for compounds } \mathbf{2} \quad (3)$$

We find that compounds **2b**−**d**, **2h**, and **2i** stand out as possessing the largest values of $\sum\Delta E_{ST}$ among compounds of both types **1** and **2**, except that **1i** is a borderline case. This finding is consistent with the notion that the value of $\Delta\Delta E_{ST}$ alone for the substituted fragment in those molecules is also a good criterion. Both of these values are presented in boldface for the five bent silenes. In comparison, the corresponding values of ΔE_{ST} are less informative.

The full optimization of $\mathbf{2b}^0$, $\mathbf{2c}^0$, $\mathbf{2d}^0$, $\mathbf{2h}^0$, and $\mathbf{2i}^0$ led to trans-bent structures (i.e., **2b**, **2c**, **2d**, **2h**,and **2i**), as given in Table 2. In the last column, we define the inversion barrier E_a to be the energy difference between the planar and bent configurations. In comparison with the planar structure, the bent structure is accompanied by a significant increase in the C=Si bond length and an increase in the Si−H length, but a decrease in the length of the carbon−substituent (C−R) bond. This finding can be rationalized by considering that the stronger covalent C−Si double bond in the planar geometry evolves into a weaker donor−acceptor-type interaction in the bent conformation. The emerging nonbonding orbital on the SiH_2 fragment in the bent conformation possesses increasing 3s character. Therefore, the Si−H bonds decrease in their 3s character and increase in their bond distance. In addition, the π orbital on the carbene fragment (R_2C) in the trans-bent conformation becomes increasingly more vacant and more available for π-donor interactions from the substituent R, which results in the contraction of the R−C bond that is depicted clearly by the resonance structure in Scheme 2.

The structures of the bent silenes that have a large degree of pyramidalization at the silicon atom and near-planar geometries at the carbon atom (indicated by $\sum\theta_{Si}$ and $\sum\theta_C$, respectively; Table 2) are consistent qualitatively with the existence of the bonding mode III in Scheme 3. In fact, there is a slight bending, with small values of δ_C, on the carbene fragments. It is clear that the trend of the folding angles at the silicon sites (δ_{Si}; **2d** > **2c** > **2b**) is consistent with the π-donating ability of the substituents (i.e., NH_2 > OH > F). This finding illustrates an interesting next-neighbor effect that the π-donor ability of the substituent R on the carbon atom has upon the SiH_2 geometry. In the next section, we demonstrate that the π donors actually push the polarized π electrons toward the silicon atom in the planar geometry.

3.2. Reversed Polarization Effect and Localization of Transition Density $\pi\sigma^*$. Even more noteworthy than the results above are the results of our natural bond orbital (NBO) analysis[39−41] of the planar silenes (Table 3). The σ bonds are strongly polarized toward the carbon atom (ca. 70%) and are nearly independent of the substituent, but the electron density distribution of the π bonds is more sensitive to the substitutents (i.e., **2h** has 61% π-electron density at its silicon atom, whereas **1h** has only 27%). π-Donating substituents at the silicon atom induce the π electrons to relocate from the silicon atom to the carbon atom; the reverse is true for π-donating substituents at the carbon atom. It appears again that first-row π-donating substituents at the carbon atom are more effective simply because of stronger π-bonding between the two first-row elements. From the orbital energy interaction diagram displayed in Figure 1, we find that π-donating

(39) Reed, A. E.; Weinstock, R. B.; Weinhold, F. *J. Chem. Phys.* **1985**, *83*, 735.
(40) Reed, A. E.; Curtiss, L. A.; Weinhold, F. *Chem. Rev.* **1988**, *88*, 899.
(41) Foster, J. P.; Weinhold, F. *J. Am. Chem. Soc.* **1980**, *102*, 7211.

Table 3. Polarization of σ_{C-Si} and π_{C-Si} Bonds as Determined from NBO Analysis (B3LYP/cc-pVDZ level) of the Atomic Charge Populations of the Planar Silenes

	polarization %	
	σ_{C-Si}	π_{C-Si}
compound	C:Si	C:Si
1a	69:31	61:39
1b	70:30	71:29
1c	70:30	73:27
1d	70:30	72:28
1e	69:31	65:35
1f	69:31	66:34
1g	70:30	61:39
1h	68:32	73:27
1i	67:33	70:30
	polarization %	
	σ_{C-Si}	π_{C-Si}
compound[a]	C:Si	C:Si
2a	69:31	61:39
2b^0	70:30	**53:47**
2c^0	71:29	**52:48**
2d^0	72:28	**46:54**
2e	74:26	64:36
2f	73:27	65:35
2g	73:27	65:35
2h^0	74:26	**39:61**
2i^0	74:26	**50:50**

[a] The symbol **2x**^{0} represents the enforced planar conformation for the fully optimized molecule **2x** of bent geometry (Table 2).

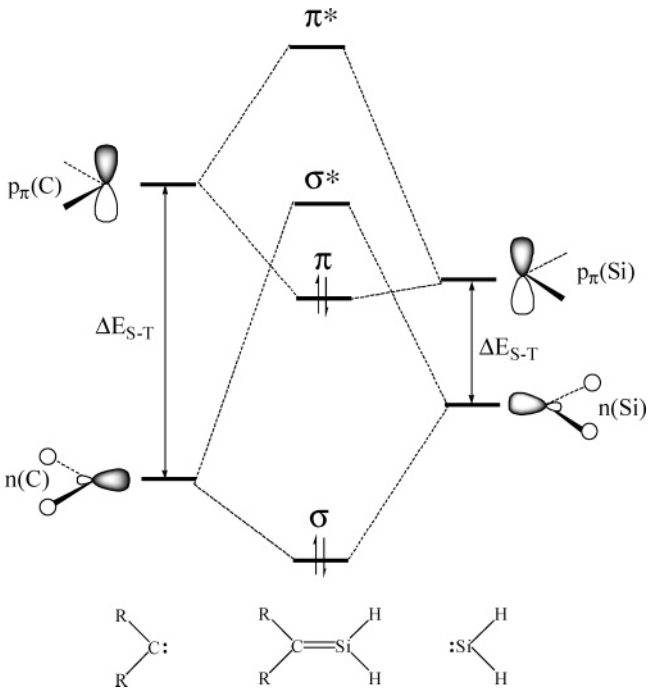

Figure 1. π-Electron-donating substitutents at the carbon atom raise the p_π level of the carbene fragment and, thus, shift the π-orbital charge toward the silicon atom. These substituents also reduce the energy gap between the π and σ^* orbitals, which, thus, provides the driving force for the SOJT effect. The equivalence between ΔE_{ST} and the gap between the p_π and n orbitals is assumed (see refs 23 and 24 for details).

substituents at the carbon atom can raise the p_π level of the carbene fragment effectively, as indicated by the value of ΔE_{S-T}. The higher level of p_π for the carbon atom relative to the silicon atom results in the polarization of the π orbital toward the silicon atom. Indeed, we find that the relative positions of the p_π levels for the singlet carbene fragments in **2b**^{0}, **2c**^{0}, **2d**^{0}, **2h**^{0}, and **2i**^{0} relative to that of SiH_2 are 2.20, 3.37, 4.63, 4.63, and 3.40 eV, respectively, as given in the last column in Table 4 [p_π(C)−p_π(Si)]. The result here is consistent qualitatively with the orbital interaction diagram sketched in Figure 4B of Ottosson's paper.[25] Figure 1 also indicates that the increase of p_π at the carbon atom also has the important consequence of reducing the gap between the π and σ^* energies, which results in their effective mixing and, thus, provides a driving force for the bending from planarity. Malrieu and Trinquier provided a general analysis for the occurrence of the geometric distortions for a broad set of unsaturated compounds.[24] This orbital mixing argument is simply based on the second-order Jahn−Teller (SOJT) effect.[42–44] Although the π and σ^* orbitals have different symmetries in the planar geometry, upon pyramidalization the two orbitals have the same symmetry and can interact with one another. Another possible mixing is that of the σ orbital with the π^* orbital, which is less important for the corresponding larger energy gap. Perturbation theory provides a convenient framework for discussing orbital interactions. The stabilization energy (E_a) due to π/σ^* orbital mixing is given qualitatively by

$$E_a \approx \langle \pi|H|\sigma^*\rangle^2/(E_\pi - E_{\sigma^*}) \qquad (4)$$

where E_π and E_{σ^*} are the orbital energies of π and σ^*, respectively. Our calculations indicate that the orbital energy difference is almost constant for **2b**−**d**, **2h**, and **2i** (ca. 11.0 eV). Thus the values of E_a depend on the square of the interaction integral (i.e., $\langle \pi|H|\sigma^*\rangle^2$), which can be large only if π and σ^* have substantial magnitudes in the same regions. Because the localization of the σ orbital is dominant on the carbon atom, the σ^* orbital is dominant on the silicon atom (ca. 70%). For **2b**−**d**, **2h**, and **2i**, the π-electron density is more localized on the silicon atom than it is on the carbon atom, as indicated in boldface in Table 3. This feature is an important difference between the five bent silenes and all the stable planar silenes (**1a**−**i** and **2e**−**g**). Because the σ^* distribution is nearly constant among all of these silenes, the π-electron density at the silicon atom correlates linearly with the values of E_a (i.e., R = 0.98) for the five bent silenes, as indicated in Figure 2. The order of the values of E_a is also consistent with the orders of both the folding angles (δ_{Si}) and the degrees of pyramidalization ($\sum\theta_{Si}$) listed in Table 2. From this analysis, we demonstrate the local contributions of $\pi-\sigma^*$ mixing for the general case of the SOJT effect for the bent heavy alkenes reported by Malrieu and Trinquier.[24] We emphasize the importance of the localization of the transition density $\pi\sigma^*$ at the silicon atom, which gives rise to its local strongly pyramidal structure. Note that we focused on the π-electron density of the enforced planar silenes; similarly, Ottosson[18] emphasized the correlation between the extent of pyramidalization and the net charge on the silicon atom in the bent geometry.

(42) Grev, R. S. *Adv. Organomet. Chem.* **1991**, *33*, 125.
(43) Cherry, W.; Epiotis, N.; Borden, W. T. *Acc. Chem. Pes.* **1977**, 167.
(44) Liang, C. X.; Allen, L. C. *J. Am. Chem. Soc.* **1990**, *112*, 1039.

Table 4. Frontier Orbital Energies in eV of Carbene and Silylene Fragments in Their Singlet States Obtained at the HF/cc-pVDZ//B3LYP/cc-pVDZ Level; the Results Obtained at the B3LYP/cc-pVDZ//B3LYP/cc-pVDZ Level Are Provided in Parentheses

	CR_2		SiH_2		energy gaps		
	n(C)[a]	p_π(C)[a]	n(Si)[a]	p_π(Si)[a]	p_π(Si) − n(C)[a]	p_π(C) − n(Si)[a]	p_π(C) − p_π(Si)[a]
2b	−12.99 (−8.26)	2.46 (−2.32)	−9.21 (−6.62)	0.26 (−3.25)	13.25 (5.01)	11.67 (4.30)	2.20 (0.93)
2c	−10.70 (−6.84)	3.64 (−0.29)	−9.21 (−6.62)	0.26 (−3.25)	10.97 (3.59)	12.84 (6.33)	3.37 (2.96)
2d	−9.13 (−5.27)	4.89 (1.37)	−9.21 (−6.62)	0.26 (−3.25)	9.40 (2.02)	14.10 (7.99)	4.63 (4.62)
2h	−8.68 (−5.64)	4.89 (1.03)	−9.21 (−6.62)	0.26 (−3.25)	8.94 (2.39)	14.10 (7.65)	4.63 (4.28)
2i	−10.02 (−6.29)	3.67 (−0.94)	−9.21 (−6.62)	0.26 (−3.25)	10.29 (3.04)	12.88 (5.68)	3.40 (2.31)

[a] See Figure 1 for the definitions of n(Si), n(C), p_π(Si), and p_π(C).

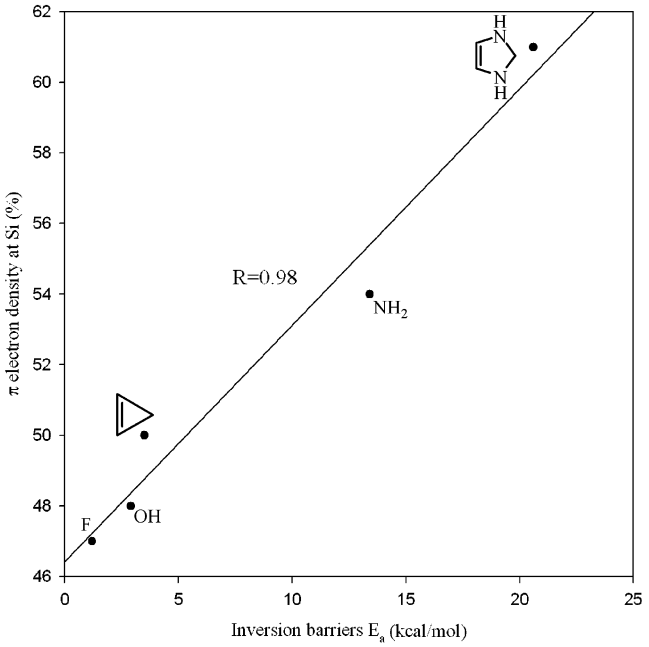

Figure 2. Correlation between the inversion barriers E_a and the π-electron density of the π bond at the Si atom for the enforced planar conformations of compounds **2b**^{0}, **2c**^{0}, **2d**^{0}, **2h**^{0}, and **2i**^{0}.

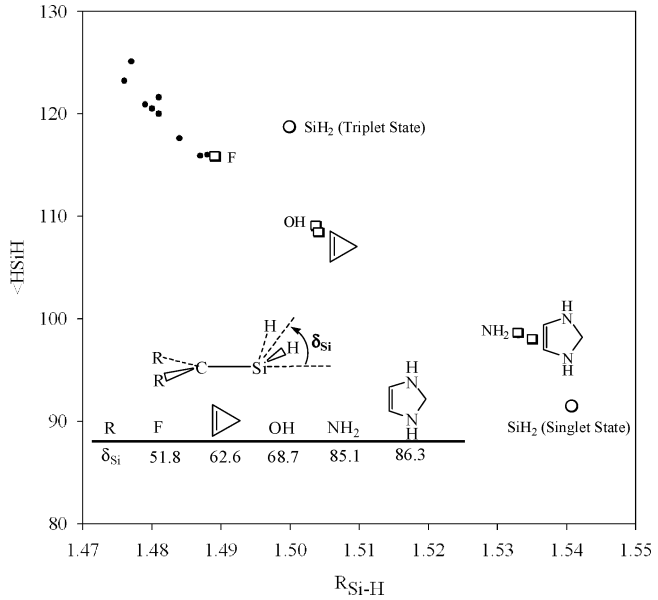

Figure 3. Two-dimensional plot of the bond lengths R_{Si}−H and the bond angles ∠HSiH of the SiH_2 fragment. For the planar compounds of type **2** in Scheme 4, including enforced planar ones, these values are represented by the dots on the upper-left side. All of these values closely resemble those of the structure of the free triplet silylene (upper open circle). The structures of the SiH_2 fragment of the bent compounds (**2b**−**d**, **2h**, and **2i**), represented by open squares, approach the structure of singlet silylene (lower open circle) as the folding angle δ_{Si} increases in this series.

3.3. Interfragmental HOMO−LUMO Interaction. The SOJT effect we discussed above emphasized the driving force for the local bending motion from a planar structure at the silicon atom. The terms π and σ^* refer to the orbitals of the planar silenes. We may also rationalize the final bent structure of bonding mode III in Scheme 3 from the frontier orbital energy information of the dissociation limits of the carbene and silylene fragments in their singlet states (Table 4). We present the Hartree−Fock results along with the B3LYP results, because of the lack of physical relevance of the virtual Kohn−Sham orbital.[45,46] Considering the constituent fragments (R_2C and SiH_2) of $R_2C{=}SiH_2$, the gap of the Hartree−Fock results between the two interacting orbital pairs [n(C), p_π(Si)] of the donor−acceptor interaction is generally smaller than that of the alternative pair [n(Si), p_π(C)], by 1.87−5.16 eV, with an exception of the **2b** system, which has the lowest inversion barrier (Table 2). Therefore, the local pyramidal structure at SiH_2 can be interpreted qualitatively as being the result of a dominant [n(C), p_π(Si)] donor−acceptor interaction.[46]

3.4. Structure of SiH_2 Fragment and CGMT Model. We note that the structural parameters of the SiH_2 fragment in the planar conformations of type **2** given in Table 1 fall within a narrow range of bond lengths (1.476−1.488 Å) and bond angles (115.9−125.1°) that are quite close to the values (1.499 Å and 118.8°) for the triplet silylene (Figure 3). In the trans-bent conformations of **2b**−**d**, **2h**, and **2i**, however, the SiH_2 fragments have singlet silylene-like structures. As a function of the folding angle (δ_{Si}), the larger the value of δ_{Si}, the closer the resemblance. For example, increasing the values of δ_{Si} for **2b**, **2i**, **2c**, **2d**, and **2h** leads to the corresponding values of R_{Si}−H (Table 2) of 1.489, 1.504, 1.504, 1.533, and 1.535 Å (cf. 1.541 Å for singlet SiH_2). The corresponding ∠HSiH bond angles are 115.8°, 108.8°, 108.5°, 98.4°, and 97.9° (cf. 91.4° for singlet SiH_2), as indicated in Figure 3. Thus, as the silene molecule distorts from a planar to trans-bent structure, the SiH_2 fragment gradually adopts a singlet silylene-like structure. In this study, we have compared

(45) Stowasser, R.; Hoffmann, R. *J. Am. Chem. Soc.* **1999**, *121*, 3414.
(46) We thank one of the referees for calling our attention to this point. We also thank the other referee for pointing out that the discussion based on the results of Table 4 is not so reliable, since the DFT and HF calculations are limited to describe an occupied-orbital energy.

the structures of the perturbed silylenes upon rehybridization (bonding with carbenes to form silenes) with those of the free structures; therefore, the match can be only qualitative. Nevertheless, our results are in accord with the general picture of the CGMT model that was designed originally for homonuclear systems; that is, the planar ethylene consists of two triplet carbene fragments (mode I in Scheme 1), and the trans-bent structure of the disilene consists of two singlet silylene fragments (mode II in Scheme 1). In this study, we have the case of a heteronuclear silene system in which bending occurs on only one side as a result of one-way donor−acceptor interactions between the singlet carbene fragment R_2C and the singlet silylene fragment SiH_2 (mode III in Scheme 3).

For the type **1** compounds, they are all planar, as a result of covalent bonding between the two triplet fragments according to the CGMT model. The structures of the local CH_2 fragments in the molecules are shown in Table 1 with the range of C−H bond lengths (1.091−1.094 Å) and bond angles (115.9−119.5°). Indeed they appear to show a greater resemblance to the triplet carbene structure than to the singlet one. Our calculated structures of the two states of CH_2 are 1.091 Å and 134.4°, and 1.126 Å and 100.3°, respectively.

4. Conclusions

The π-electron reversed-polarization effect has been utilized to enhance the kinetic stability of silenes. In this paper, we have rationalized the finding that this effect also induces the bent structure of silenes, as reported by Ottosson. π-Donor substituents at the carbon atom are effective in polarizing the π-electron charge toward the silicon atom. The SOJT effect is useful when rationalizing the connection between such reversed-charge polarization and the bending of the silylene fragment away from its planar conformation with an important localization of the transition density $\pi\sigma^*$. The bent geometries of silenes also can be understood directly from a consideration of the two competing HOMO−LUMO interactions between the CR_2 and SiH_2 fragments. We also find that the locally bent structure of the SiH_2 fragment can be interpreted in terms its valence state, from triplet to singlet, dependent on the folding angle δ_{Si}, which is in accord with the CGMT model. Thus, this model also holds for mixed-row silene compounds. Therefore, the silene series $R_2C{=}SiH_2$ that we studied here displays an interesting bonding pattern continuum—from covalent to dative C−Si bonds (bonding mode I to mode III)—that is controlled by the π-donor ability of the substituent R on the carbon atom.

Acknowledgment. This work was supported by the National Science Council of Taiwan, Republic of China. We thank the National Center for High-performance Computing for computer time and facilities. We thank the two reviewers for their helpful suggestions to improve the manuscript.

Supporting Information Available: This material is available free of charge via the Internet at http://pubs.acs.org.

OM050221J